Eur. Phys. J. E **23**, 281–287 (2007)
DOI 10.1140/epje/i2007-10189-0

THE EUROPEAN PHYSICAL JOURNAL E

Deduction of the temperature-dependent structure of the four-layer intermediate smectic phase using resonant X-ray scattering

P.D. Brimicombe[1], N.W. Roberts[1], S. Jaradat[1], C. Southern[1], S.-T. Wang[2], C.-C. Huang[2], E. DiMasi[3], R. Pindak[3], and H.F. Gleeson[1,a]

[1] School of Physics and Astronomy, University of Manchester, Manchester, M13 1PL, UK
[2] School of Physics and Astronomy, University of Minnesota, Minneapolis, MN 55455, USA
[3] Brookhaven National Laboratory, NSLS - Upton, NY 11973, USA

Received 23 April 2007
Published online: 20 July 2007 –

Abstract. A binary mixture of an antiferroelectric liquid-crystal material containing a selenium atom and a highly chiral dopant is investigated using resonant X-ray scattering. This mixture exhibits a remarkably wide four-layer intermediate smectic phase, the structure of which is investigated over a temperature range of 16 K. Analysis of the resonant X-ray scattering data allows accurate measurement of both the helicoidal pitch and the distortion angle as a function of temperature. The former decreases rapidly as the SmC^* phase is approached, whilst the latter remains constant over the temperature range studied at $8° \pm 3°$. We also observe that the senses of the helicoidal pitch and the unit cell of the repeating four-layer structure are opposite in this mixture and that there is no pitch inversion over the temperature range studied.

PACS. 61.30.Eb Experimental determinations of smectic, nematic, cholesteric and other structures – 78.70.Ck X-ray scattering – 83.80.Xz Liquid crystals: nematic, cholesteric, smectic, discotic, etc.

1 Introduction

Smectic liquid-crystal phases possess short-range positional order of the molecules in a layered structure and orientational order of the molecules within each layer, but no long-range positional order. In the polar tilted smectic phases, the long axes of the molecules within each layer are tilted with respect to the layer normal, with a spontaneous polarisation perpendicular to both the layer normal and the tilt direction. The most common polar tilted smectic phase is the chiral smectic C phase (SmC^*) shown in Figure 1, in which the chirality eliminates the symmetry along the mirror plane parallel to the layer normal and the tilt direction, producing the spontaneous polarisation [1]. This phase is commonly described as being ferroelectric, though the chirality produces a macroscopic helicoidal structure, the period of which is typically of the order of several hundred nanometres, corresponding to hundreds of smectic layers. When attempting to synthesise materials of very high spontaneous polarisation, the antiferroelectric phase (SmC^*_A), in which the direction of molecular tilt reverses in adjacent smectic layers, was discovered [2] (see Fig. 1). Since the direction of spontaneous polarisation reverses from one smectic layer to the next, this phase is non-polar. The discovery of the antiferroelectric phase was of great interest since its properties allowed novel switching modes to be seen in thin-film electro-optic devices, potentially solving many of the problems associated with ferroelectric liquid crystal devices [2].

In the process of investigating materials that form the antiferroelectric phase, at least two more tilted smectic phases, known as the *intermediate* smectic phases, were observed between the SmC^* and SmC^*_A [3–5]. The general phase sequence when increasing the temperature is $SmC^*_A \leftrightarrow SmC^*_{FI1} \leftrightarrow SmC^*_{FI2} \leftrightarrow SmC^* \leftrightarrow SmC^*_\alpha \leftrightarrow SmA$, though some of these phases will be absent in some systems. The SmC^*_α phase is a chiral tilted smectic phase that has a structure in which the helicoidal pitch is of the order of only a few layers [6, 7], compared to some hundreds of layers in the other phases.

Until recently there has been considerable debate as to the structure of the intermediate smectic phases SmC^*_{FI1} and SmC^*_{FI2}, but they have since been confirmed to have unit cells of three layers and four layers, respectively [6]. The labelling of these phases is somewhat inconsistent, so we will refer to them simply as the three- and four-layer intermediate smectic phases. Considerable effort has been made to find the precise structure of these phases, with

[a] e-mail: helen.gleeson@manchester.ac.uk

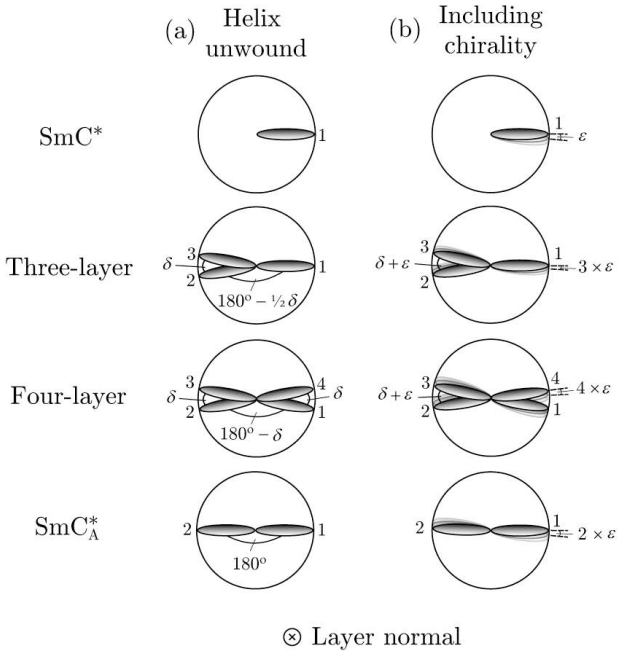

Fig. 1. The structure of the tilted smectic phases as viewed along the layer normal (temperature decreases from top to bottom). (a) When the influence of the macroscopic helicoidal pitch is not shown, the unit cell of each phase can be observed. The three- and four-layer intermediate smectic phases are characterised by a distortion angle, δ. (b) The chirality of the phase induces a step change in the azimuthal angle from one layer to the next of ε, with the magnitude of ε being both temperature and phase dependent. In the system shown above, the senses of the macroscopic helix and the unit cells of the three- and four-layer intermediate smectic phases are the same. Note that the intermediate phases have not been observed in the absence of chirality.

resonant X-ray scattering providing the most reliable and direct information [6–11], though other methods have also been used with some success [12, 13]. These studies have concluded that the structure of the intermediate phases follows the distorted clock model [14] shown in Figure 1. Both the three- and four-layer phases are characterised by the long-range helicoidal pitch, P and by a distortion angle, δ, which specifies the degree of biaxiality in the system (the parameter ε in Figure 1 derives from the helicoidal pitch). It is interesting to note that only the three-layer phase is truly ferrielectric since, due to its symmetry, the four-layer phase has no bulk spontaneous polarisation, and could be considered antiferroelectric.

Whilst the structure of these phases has now been verified, the variation of this structure with temperature is only now being investigated, with the various theoretical models that have been proposed predicting different behaviours. The distortion angle of the three-layer phase has been shown experimentally to be temperature independent, while the pitch increases approximately linearly with temperature [10]. Although Cady *et al.* measured the distortion angle of the four-layer phase at three discrete temperatures using resonant X-ray scattering and found no significant variation beyond experimental error, no information was presented regarding the temperature variation of the helicoidal pitch and the temperature range investigated was small [9]. Measurements of the optical rotatory power of free-standing films by Čepič *et al.* indicate divergence of the helicoidal pitch in the four-layer phase followed by pitch inversion as the temperature is increased [13].

In addition to this experimental work, two distinct theoretical models for these phases have been developed. In the first model, it is the interaction between the elastic forces and the flexoelectric and spontaneous polarisations that causes formation of the intermediate phases [13, 15–17]. While Čepič *et al.* and Olson *et al.* assume that direct dipole interactions between next-nearest neighbouring smectic layers are important but that indirect long-range interactions are unimportant [13, 15, 17], Emelyanenko and Osipov include only direct interactions between adjacent smectic layers but allow indirect long-range interactions [16]. These two sets of assumptions appear to make little difference to the phase structures predicted, however. Čepič *et al.* assume that the effective quadrupolar coupling is proportional to $(T - T_c)$, where T_c is the transition temperature from SmA to SmC* [13], causing the distortion angle in the four-layer intermediate phase to vary considerably with temperature. Olson *et al.* and Emelyanenko and Osipov, however, assume that the effective quadrupolar coupling remains constant with temperature, and predict a constant distortion angle in this phase. In the second theoretical model, proposed by Hamaneh and Taylor, a combination of dynamic flexing of the smectic layers due to thermal fluctuations and the elastic anisotropy of this type of deformation has been shown to induce both commensurate and incommensurate repeating layer structures [18]. No predictions as to the temperature dependence of either the distortion angle or the helicoidal pitch have been made using this model, however.

In this paper we present detailed measurements of both the helicoidal pitch and distortion angle of the four-layer phase over a temperature range of 16 K using resonant X-ray scattering.

2 Resonant X-ray scattering

Although small angle X-ray scattering has proved to be a reliable tool in determining the phase structure of many liquid crystalline systems, it is of limited use in the case of the intermediate smectic phases since it only provides information about the spacing and orientation of the smectic layers, giving no information about the molecular orientation within each layer. In resonant X-ray scattering, the energy of the incident beam is tuned to the absorption edge of a suitable atom in the material under investigation, in this case a selenium atom. Under these conditions, it has been shown that the structure factor becomes a tensor, leading to the presence of reflections that would otherwise be forbidden, and these reflections are sensitive to molecular orientation [19]. The tensorial structure factor for smectic liquid-crystal phases was formulated by

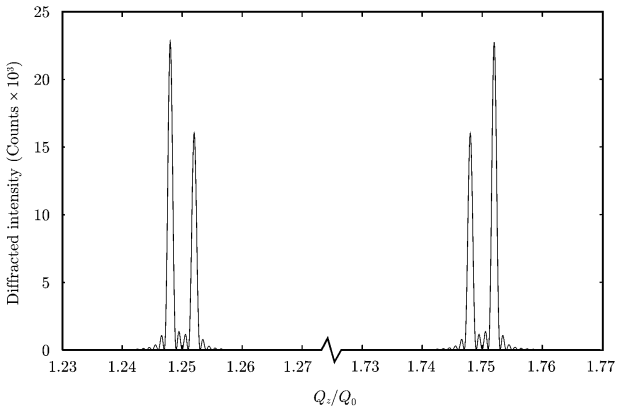

Fig. 2. Calculated π-polarised first-order diffraction peaks for the four-layer intermediate smectic phase with $\delta = 10°$ and $P = 500$ layers. The resonant peaks are centred about the 1.25 and 1.75 positions because of the periodicity of the phase. The separation of each pair of peaks depends on the helicoidal pitch while the relative intensity of each pair is determined by the distortion angle. In these calculations, the senses of the helicoidal pitch and the unit cell are opposite.

Levelut and Pansu [20] and this has been widely used to interpret the results of resonant X-ray scattering experiments carried out on the intermediate phases [7, 9–11]. According to this theory, resonant peaks should be observed at the following positions:

$$\frac{Q_z}{Q_0} = l + m\left(\frac{1}{\nu} \pm \varepsilon\right), \qquad (1)$$

where Q_0 is the scattering vector of the Bragg peak, l and m are positive or negative integers whose moduli are less than or equal to two, ε is the ratio of the helicoidal pitch and the smectic layer spacing and ν is the number of layers in the unit cell, *i.e.* $\nu = 4$ in the case of the four-layer phase.

An example of the resonant diffracted peaks near the $Q_z/Q_0 = 1.25$ and 1.75 positions for a four-layer phase of the structure shown in Figure 1 is shown in Figure 2. Only first order ($m = \pm 1$) peaks are present at these positions, and while second order ($m = \pm 2$) peaks might be expected near the $Q_z/Q_0 = 1.5$ position, none were seen experimentally in this system (note that resonant peaks at this position have been observed previously, but that they are typically orders of magnitude smaller than the first-order peaks at the 1.75 position [7]). We have also confirmed by polarisation analysis of the scattered X-ray intensity that only first-order resonant peaks are observed in the three-layer phase of a similar system. The second-order peaks are not seen in either case because they are attenuated by thermal fluctuations in the molecular orientation to a far greater extent than the first-order peaks [10].

The precise shape and position of the resonant peaks provide information about the structure of the phase. The periodicity of the phase defines the centres of the resonant peak pairs, leading to centres at the 1.25 and 1.75 positions in the four-layer phase. The separation of each pair of peaks is due to the helicoidal pitch (*i.e.* due to ε in Eq. (1)), with a shorter pitch producing a larger separation. The fact that the peaks in each pair are not of equal magnitude indicates that the phase is biaxial, and so the intensity ratio depends on the distortion angle. If $\delta = 0°$ (the Ising model) the resonant peaks are of equal magnitude, and if $\delta = 90°$ (the clock model), the smaller peak of each pair disappears. In addition, if the smaller peak is closer to the $Q_z/Q_0 = 1.5$ position, then the senses of the helicoidal pitch and the unit cell are opposite, as can be seen in the example shown in Figure 2. If this is not the case, these two properties have the same handedness.

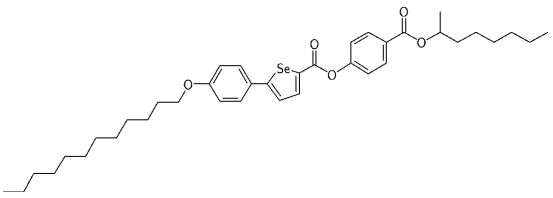

Fig. 3. The chemical structure of component AIS179. This material is mixed with 6 wt% of chiral dopant R1011 (Merck) and during the experiments, the X-ray energy is tuned to the K-absorption edge of the selenium atom contained in the core of the liquid crystalline component.

3 Experiment

The material under investigation is a binary mixture of R-handed antiferroelectric liquid crystal AIS179, shown in Figure 3, and 6 wt% of chiral dopant R1011 (Merck). Some of the properties of this mixture have been reported previously [21] and it is of particular interest in this instance since it possesses a very wide four-layer intermediate smectic phase. Its phase transition temperatures, determined using a combination of optical microscopy on free-standing films and devices and small-angle X-ray scattering, are

$$\underset{}{\mathrm{I}} \underset{114.0\,^\circ\mathrm{C}}{\longrightarrow} \mathrm{SmA} \underset{85.9\,^\circ\mathrm{C}}{\longrightarrow} \mathrm{SmC}^* \underset{70.8\,^\circ\mathrm{C}}{\longrightarrow} \mathrm{SmC}^*_{\mathrm{FI2}} \underset{33.0\,^\circ\mathrm{C}}{\longrightarrow} \mathrm{Cr} \quad ,$$

where I stands for the isotropic liquid phase, and Cr the crystalline solid. It should be noted that the presence of a SmC^*_α phase between the SmA and SmC^* phases cannot be ruled out because of the difficulty in identifying its optical texture, particularly since the molecular tilt is small in this mixture [21].

The resonant X-ray scattering experiments were carried out at Station X6B of the National Synchrotron Light Source, Brookhaven National Laboratories, NY, USA. A synchrotron radiation source is required for resonant X-ray scattering since the energy must be tuned accurately to the absorption edge of the appropriate atom, and high flux is required since the liquid-crystal samples used are typically very thin when compared to bulk samples, and only weakly scattering. In these experiments, the energy of the source was tuned to the K-absorption edge of the selenium atom contained within the core of the AIS179 component (this absorption edge was found by carrying out an energy scan on a powder sample of

pure AIS179). The X-ray energy was then optimised at 12.6565 keV by incrementing the energy in small steps so as to achieve the maximum signal to noise ratio once a set of resonant peaks had been found. Such fine adjustment of the X-ray energy is required, since the resonant signal is only present over a range of ~ 9 eV.

Free-standing films a few microns in thickness were prepared by slowly dragging a thin glass spreader across an elliptical hole measuring 10 mm by 5 mm in a metal plate. Such large films are required since although the aperture of the X-ray beam is only 0.3 mm by 0.4 mm in cross-section, the beam is positioned at grazing incidence to the film, leading to a very large footprint (the incident angle is typically $1-2^\circ$). The films were held in a double-stage temperature-regulated oven whose temperature stability is around 0.01 °C, with a polarising microscope assembly allowing observation of the film *in situ* whilst the measurements were being taken. In order to obtain good alignment of the smectic layers with the layer and film normals parallel, films were spread at a temperature just above the SmA to SmC* transition. After spreading, the oven system was flushed with helium in order to reduce the effects of air scatter. Since the X-ray beam can seriously damage the liquid-crystal material, no film was used for measurement at more than two temperatures. In order to check for beam damage, the Bragg peak at the $Q_z/Q_0 = 2$ position was examined since any splitting of this peak will be solely due to damage to the film.

Only the resonant peaks at the 1.75 position are investigated in this paper since the proximity of the 1.25 position to the Bragg peak at $Q_z/Q_0 = 1$ causes the baseline of the experimental data to slope significantly, adding further uncertainty to the fitting procedure described later.

4 Data analysis

In order to determine the pitch and distortion angle from the experimental data, the theory of Levelut and Pansu [20] is used to calculate the scattered intensity, which is then convolved with the resolution function of the experiment, in this case approximated by a Lorentzian. The calculations are carried out over a fine resolution in Q-space, with interpolation used to match to the resolution of the experimental data for comparison purposes. In addition, the scattered intensity and the resolution function are calculated over a sufficiently large range of Q_z/Q_0 such that there are no end errors caused by the convolution. Normalisation of the calculated intensity is achieved by matching the averages of the experimental and theoretical datasets in order to reduce the sensitivity to noise at the peak data point (this comparison is made at the experimental Q-space resolution).

The experimental data are then fitted using a grid-search algorithm, with grid resolutions of 1° in the distortion angle and one smectic layer in the helicoidal pitch. The temperature variation of the smectic layer spacing in this system has been reported previously [21], with these values used in the calculations presented here.

Since calibration of the lattice parameter of the system requires exposure of the film to the X-ray beam, repeated recalibration for changes in the layer spacing with temperature would cause considerable damage to the liquid crystal film. As the layer spacing varies only slightly over the temperature range investigated here, calibration of the lattice parameter was not performed for every measurement temperature, leading to some slight uncertainty as to the precise position of the experimental data on the Q_z/Q_0 axis. In order to account for this error in the lattice parameter (*i.e.* Q_0), a scaling factor for the Q_z/Q_0 axis has been included as a fitting parameter, with a resolution of 5×10^{-6}. As would be expected, for a fixed lattice parameter the shift is towards positive Q at lower temperatures where the layer spacing is larger (the scattering is over a smaller angle), and towards negative Q at higher temperatures where the layer spacing is smaller.

The expected error in the experimental data varies in proportion to the magnitude of the data, and so the χ^2 value has been used as the measure of fit quality, rather than the square of the absolute error:

$$\chi^2 = \sum_{i=0}^{N} \frac{(y_i - E_i)^2}{y_i}, \tag{2}$$

where y_i and E_i are the experimental and fitted data values, respectively, and the summation is performed over the entire dataset.

5 Results

The experimental resonant X-ray scattering peaks at the 1.75 position for a range of temperatures are shown in Figure 4. One immediately notes that only a single peak is discernible by eye in the experimental data, indicating that either the distortion angle is approaching 90°, in which case the second peak becomes very small, or the helicoidal pitch is long, since this causes the two peaks to overlap significantly. Since the experimental data in Figure 4 exhibit a marked asymmetry (the gradients of the rising and falling edges are significantly different), the latter case can be confirmed.

The best fits to the experimental data are also shown in Figure 4, with the excellent agreement between simulation and experiment apparent. It should be noted that the fitted peak widths are of a similar magnitude to the those at the $Q_z/Q_0 = 2$ position, though a significant increase in width is observed as the temperature is increased, due to a decrease in the order parameter as the SmC* phase is approached.

The temperature dependence of the distortion angle and helicoidal pitch found through fitting of the resonant peaks is shown in Figure 5 (the temperature is measured relative to the four-layer to SmC* phase transition temperature). The distortion angle appears to be constant at $8^\circ \pm 3^\circ$ over the temperature range investigated. Previous measurements using ellipsometry and resonant X-ray scattering have confirmed that the distortion angle is typically small ($7^\circ \pm 3^\circ$ for material MHBPC [12] and around

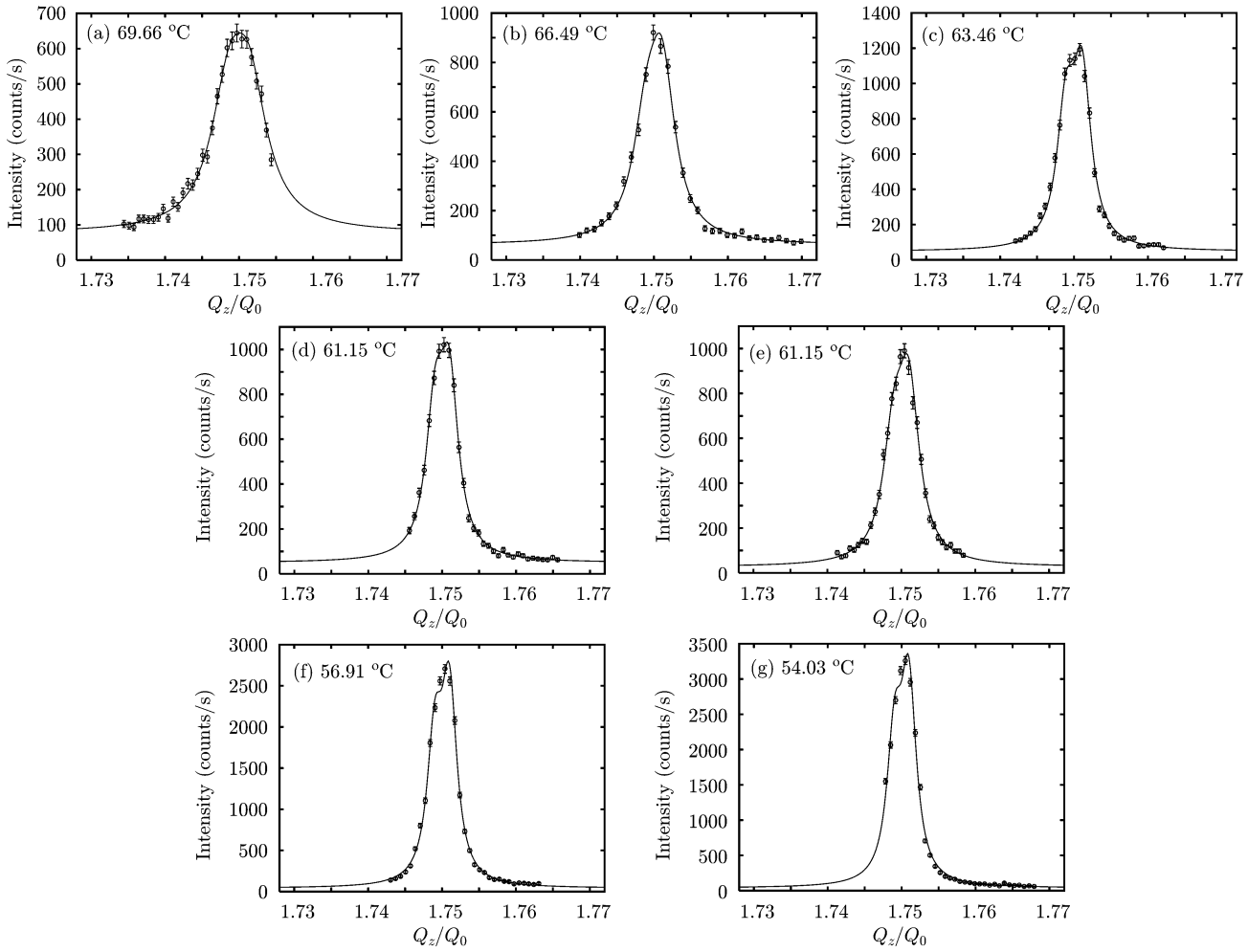

Fig. 4. Resonant X-ray scattering peaks for the four-layer phase over a range of temperatures (two datasets were taken at 61.15 °C to check the repeatability of the measurements). The experimental data are represented by points and solid lines indicate the best fit obtained.

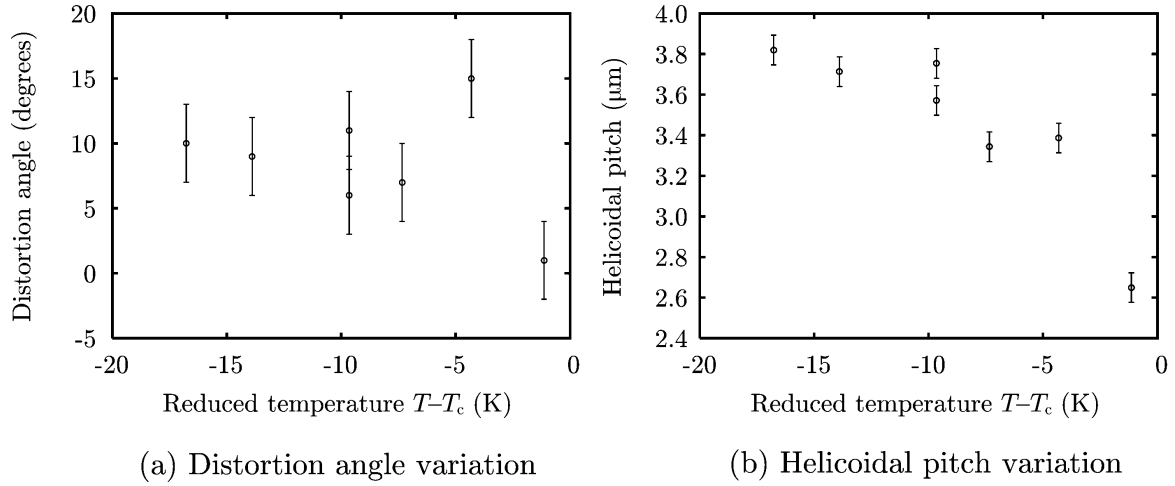

Fig. 5. The variation of (a) the distortion angle and (b) the helicoidal pitch as a function of reduced temperature (T_c is the four-layer–to–SmC*-phase transition temperature). There is no significant variation in the distortion angle over this temperature range, but the helicoidal pitch decreases rapidly close to the transition to the SmC* phase.

Table 1. The material parameters of the materials in which the distortion angle of the four-layer intermediate smectic phase, δ, has been measured (the method used to determine the distortion angle is also listed). Parameters marked * are taken from reference [21], those marked † are taken from reference [22] and those without markings are from the same source as the distortion angle measurement. The data listed for the 6% doped AIS179 are those presented in this paper, and include the temperature variation of the helicoidal pitch. The two pitch values found by Johnson *et al.* for MHDDOPTCOB are for free-standing films of different thicknesses [12]. N/A indicates that data were not readily available in the literature.

Material	P_s (nC/cm^2)	Optical tilt θ	$\frac{P_s}{\sin\theta}$	Pitch (μm)	Distortion angle δ	Measurement method
MHPBC	N/A	11°	N/A	4	7°	Ellipsometry [12]
6% doped AIS179	70*	24°*	170	2.6 to 3.8	8°	Resonant X-ray scattering
3% doped AIS179	100*	28°*	210	2.9	14°	Resonant X-ray scattering [10]
MHDDOPTCOB	60†	32°†	110	1.7	15-20°	Resonant X-ray scattering [9]
	60†	32°†	110	2.3 & 5.0	18°	Ellipsometry [12]
10OTBBB1M7	N/A	20°	N/A	4	26°	Optical rotatory power [13]
MHPOBC	N/A	10–12°	N/A	N/A	48°	Optical rotatory power [13]

17° ± 2° for material MHDDOPTCOB [9, 12]). As discussed previously, Cady *et al.* measured the distortion angle of material MHDDOPTCOB at three distinct temperatures, finding no significant temperature variation [9], and the same trend is observed here in a different system over a much larger temperature range.

The variation of the helicoidal pitch with temperature is shown in Figure 5(b), and clearly this parameter decreases rapidly as the SmC^* phase is approached. In addition, the pitch is generally long, which is typical of the four-layer intermediate phase (other measurements of the helicoidal pitch of this phase in different materials at isolated temperatures are 5 μm and 2.3 μm [12] and 1.65 μm [9]), while the pitch of the three-layer phase is typically somewhat shorter (around 500 nm in a similar system [10]). Helix unwinding followed by pitch inversion as the temperature is increased, as reported by Čepič *et al.* [13] and predicted by Olson *et al.* [15], is not observed in this mixture over the temperature range examined. A sudden decrease in the helicoidal pitch of the four-layer phase as a phase transition is approached is predicted by the theory of Olson *et al.*, but this result is only reported for transitions to SmC^*_α phases rather than the SmC^* phase [15].

Since the smaller peaks shown in Figure 4 are consistently closer to the 1.5 position than the larger peaks, the twist senses of the helicoidal pitch and the unit cell are opposed. The same is true for the three-layer phase of a similar system, as can be seen from Figure 3 of reference [10], in which the smaller resonant peaks are closer to the 1.5 position. Cady *et al.*, however, found that the reverse was true for the four-layer phase of MHDDOPTCOB [9].

6 Conclusions

The temperature dependence of the structure of the four-layer intermediate smectic liquid-crystal phase has been measured using resonant X-ray scattering. The four-layer intermediate smectic phase is stabilised over a large temperature range by the addition of a highly chiral dopant to an antiferroelectric liquid crystal material, allowing measurement of its properties over a range of 16 K. While the distortion angle of this phase was found to be broadly independent of temperature (corroborating previous experimental results over a smaller temperature range [9]), the helicoidal pitch decreases rapidly as the four-layer to SmC^* phase transition is approached at higher temperatures. A constant distortion angle has also been reported in the three-layer intermediate phase, though in this case the helicoidal pitch increases approximately linearly with increased temperature [10]. In addition, the experimental data indicate that the sense of rotation of the helicoidal pitch is the reverse of that of the unit cell, a phenomenon also previously observed in the three-layer phase [10]. Since the opposite has been reported for the four-layer phase of MHDDOPTCOB [9], we must conclude that the relative sense of the unit cell and the helicoidal pitch is material dependent.

If the intermediate phases are stabilised by the interaction between the elastic torque and the flexoelectric and spontaneous polarisations, the fact that the distortion angle of the four-layer phase remains constant with temperature indicates that the effective quadrupolar coupling varies little over the temperature range investigated. The assumption made by Čepič *et al.* that this coupling should be linear with $(T - T_c)$ is only valid close to the SmA to SmC^* transition temperature (T_c) [13], whereas in the mixture investigated here, formation of the four-layer phase only occurs 15 K below this temperature. This far from the transition to the tilted phases the variation of the tilt angle with temperature is small [21], producing only a small variation in the effective quadrupolar coupling, and leading to a distortion angle that does not vary significantly with temperature, as predicted by Emelyanenko and Osipov [16].

In addition, some theoretical and experimental results have indicated the possibility of helix unwinding and pitch inversion in the four-layer phase, and these phenomena have not been observed here [13, 15]. The fact that Olson

et al. predict a similar sudden decrease in the pitch close to a phase transition to that observed in this system indicates that pitch inversion may occur over a larger temperature range than has been investigated in this work [15].

Finally, we note that the reason the distortion angles in the intermediate smectic phases are non-zero is because of the presence of a chiral torque. This torque might then be expected to be dependent on one or both of the inverse pitch of the system and $P_s/\sin\theta$, where P_s is the spontaneous polarisation of the liquid crystal material and θ is the optical tilt angle. It is interesting to consider, therefore, whether there is any correlation between the distortion angle and chirality for the data available for materials that exhibit the four-layer intermediate phase. From the data readily available in the literature listed in Table 1, however, there is no obvious relationship between either of these parameters and the distortion angle. Unfortunately there are too few data at present to determine whether or not there is a coupled relationship between these two parameters and the distortion angle.

The authors would like to thank Dr M. Hird (University of Hull, UK) and Prof. J.W. Goodby (University of York, UK) for kindly providing the liquid crystal host material, and Merck Speciality Chemicals Ltd., Chilworth, UK for supplying the chiral dopant R1011. We thank Mikhail Osipov and Maxim Garkounov of the University of Strathclyde for their input via discussions. Thanks also to the EPSRC, UK for their financial support through grant number EP/D069793/1. S.-T. Wang and C.-C. Huang are supported in part by NSF grant number DMR-0106122. Use of the National Synchrotron Light Source, Brookhaven National Laboratory, was supported by the U.S. Department of Energy, Office of Science, Office of Basic Energy Sciences, under Contract No. DE-AC02-98CH10886.

References

1. R.B. Meyer, L. Liébert, L. Strzelecki, P. Keller, J. Phys. (Paris) **36**, L-69 (1975).
2. A. Chandini, E. Gorecka, Y. Ouchi, H. Takezoe, A. Fukuda, Jpn. J. Appl. Phys. **28**, L1265 (1989).
3. M. Fukui, H. Orihara, Y. Yamada, N. Yamamoto, Y. Ishibashi, Jpn. J. Appl. Phys. **28**, L849 (1989).
4. A.D. Chandani, T. Ouchi, H. Takezoe, A. Fukuda, K. Terashima, K. Furukawa, A. Kishi, Jpn. J. Appl. Phys. **28**, L1261 (1989).
5. A. Fukuda, Y. Takanishi, T. Isozaki, K. Ishikawa, H. Takezoe, J. Mater. Chem. **4**, 997 (1994).
6. P. Mach, R. Pindak, A.-M. Levelut, P. Barois, H.T. Nguyen, C.C. Huang, L. Furenlid, Phys. Rev. E **81**, 1015 (1998).
7. L.S. Hirst, S.J. Watson, H.F. Gleeson, P. Cluzeau, P. Barois, R. Pindak, J. Pitney, A. Cady, P.M. Johnson, C.C. Huang, A.-M. Levelut, G. Srajer, J. Pollmann, W. Caliebe, A. Seed, M.R. Herbert, J.W. Goodby, M. Hird, Phys. Rev. E **65**, 041705 (2002).
8. P. Mach, R. Pindak, A.-M. Levelut, P. Barois, H.T. Nguyen, H. Baltes, M. Hird, K. Toyne, A. Seed, J.W. Goodby, C.C. Huang, L. Furenlid, Phys. Rev. E **60**, 6793 (1999).
9. A. Cady, J.A. Pitney, R. Pindak, L.S. Matkin, S.J. Watson, H.F. Gleeson, P. Cluzeau, P. Barois, A.-M. Levelut, W. Caliebe, J.W. Goodby, M. Hird, C.C. Huang, Phys. Rev. E **64**, 050702 (2001).
10. N.W. Roberts, S. Jaradat, L.S. Hirst, M.S. Thurlow, Y. Wang, S.T. Wang, Z.Q. Liu, C.C. Huang, J. Bai, R. Pindak, H.F. Gleeson, Europhys. Lett. **72**, 976 (2005).
11. H.F. Gleeson, L.S. Hirst, Chem. Phys. Chem. **7**, 321 (2006).
12. P.M. Johnson, D.A. Olson, S. Pankratz, T. Nguyen, J. Goodby, M. Hird, C.C. Huang, Phys. Rev. Lett. **84**, 4870 (2000).
13. M. Čepič, E. Gorecka, D. Pociecha, B. Žeckš, H.T. Nguyen, J. Chem. Phys. **117**, 1817 (2002).
14. T. Akikzuki, K. Miyachi, Y. Takanishi, K. Ishikawa, H. Takezoe, A. Fukuda, Jpn. J. Appl. Phys. **38**, 4832 (1999).
15. D.A. Olson, X.F. Han, A. Cady, C.C. Huang, Phys. Rev. E **66**, 021702 (2002).
16. E. Emelyanenko, M.A. Osipov, Phys. Rev. E **68**, 051703 (2003).
17. M. Čepič, B. Žeckš, Phys. Rev. Lett. **87**, 085501 (2001).
18. M.B. Hamaneh, P.L. Taylor, Phys. Rev. E **93**, 167801 (2004).
19. V.E. Dmitrienko, Acta Crystallogr., Sect. A **39**, 29 (1983).
20. A.-M. Levelut, B. Pansu, Phys. Rev. E **60**, 6803 (1999).
21. S. Jaradat, N.W. Roberts, Y. Wang, L.S. Hirst, H.F. Gleeson, J. Mater. Chem. **16**, 3753 (2006).
22. J. Mills, R. Miller, H. Gleeson, A. Seed, M. Hird, P. Styring, Mol. Cryst. Liq. Cryst. **303**, 145 (1997).